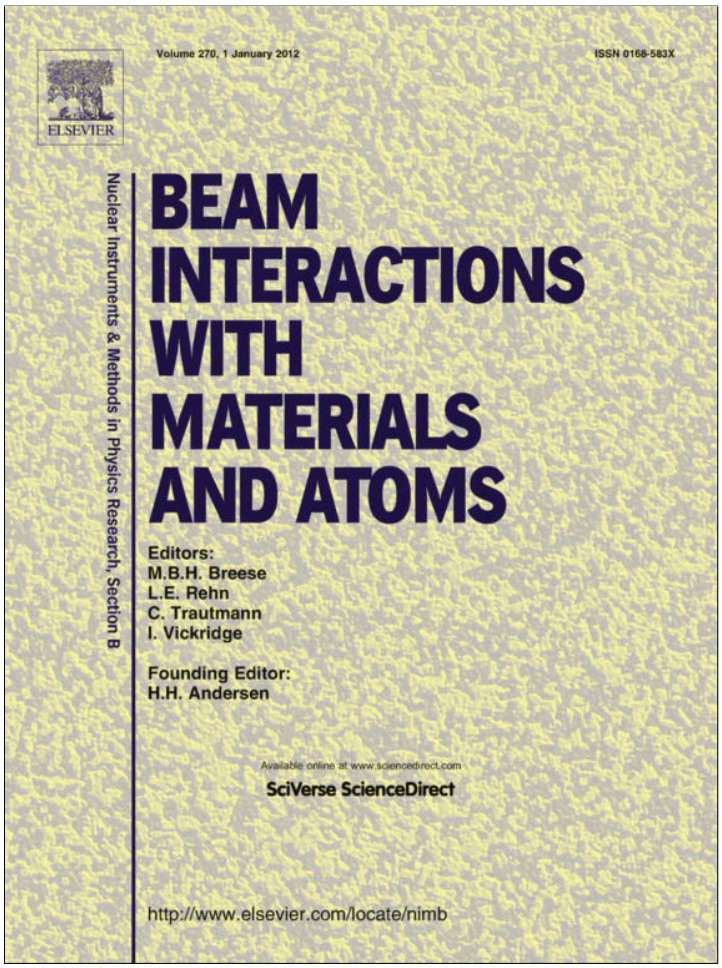

(This is a sample cover image for this issue. The actual cover is not yet available at this time.)

Nuclear Instruments and Methods in Physics Research B 278 (2012) 8–14

Contents lists available at SciVerse ScienceDirect

Nuclear Instruments and Methods in Physics Research B

journal homepage: www.elsevier.com/locate/nimb

Analysis of early medieval glass beads – Glass in the transition period

Žiga Šmit [a,b,*], Timotej Knific [c], David Jezeršek [b], Janka Istenič [c]

[a] Faculty of Mathematics and Physics, University of Ljubljana, Jadranska 19, SI-1000 Ljubljana, Slovenia
[b] Jožef Stefan Institute, Jamova 39, P.O.B. 3000, SI-1001 Ljubljana, Slovenia
[c] National Museum of Slovenia, Prešernova 20, SI-1000 Ljubljana, Slovenia

ARTICLE INFO

Article history:
Received 12 August 2011
Received in revised form 30 January 2012
Available online 14 February 2012

Keywords:
Sodium glass
Natron
Halophytic plants
PIXE
PIGE

ABSTRACT

Glass beads from graves excavated in Slovenia and dated archaeologically to the 7th–10th century AD were analysed by the combined PIXE–PIGE method. The results indicate two groups of glass; natron glass made in the Roman tradition and glass made with alkalis from the ash of halophytic plants, which gradually replaced natron glass after *c.* 800 AD. The alkalis used in the second group of glass seem to be in close relation to a variant of the Venetian white glass that appeared several centuries later. The origin of this glass may be traced to glass production in Mesopotamia and around the Aral Sea. All the mosaic beads with eye decoration, as well as most of the drawn-segmented and drawn-cut beads analysed, are of plant-ash glass, which confirms their supposed oriental origin.

1. Introduction

Roman and post-Roman glassmaking was specialised and regionalised, allocating production of raw glass to the geographical area of Egypt and Palestine [1]. Raw glass was produced in huge blocks, exploiting local siliceous sand from the coast, naturally enriched by calcium from sea shells, and the alkali sediments from Egyptian wadis; this is known today as natron [2]. These two components provided all the necessary ingredients of glass: a siliceous matrix (with Ca as stabiliser) and a relatively pure alkali flux. Chunks of raw glass were then distributed, mainly through sea trade, to the secondary workshops where they were reworked into final products. Local treatment also included decolouration and pigmentation. The influence of impurities, which mainly originated from the sand component, was neutralised by decolourisers, typically manganese and antimony oxides [3].

The present state of research suggests that political events in Egypt, starting with the Persian invasion in 619, continuing with a complex Muslim–Christian conflict in the 7th and 8th centuries, and the Berber invasion in the 9th century, strongly disturbed access to natron sources [4]. As a response, a new technology of obtaining alkalis was developed in the Byzantine or/and Islamic world. Alkalis with a large fraction of sodium were obtained from the ash of halophytic plants. In the past, plant ash had already been used in Bronze Age Egyptian and Mesopotamian glassmaking [5].

The transition to the new alkali source was not immediate, especially as large quantities of natron-type glass were circulating in the former Roman world [6]. Natron-type glass was identified in Late Roman/Early Christian centres, like San Martino di Ovaro in Northern Italy [7], Jarrow in England [2] and Tonovcov grad in Slovenia [8]. The glass beads in circulation in the Merovingian kingdom (middle of the 5th – middle of the 8th century) were also of the natron-type [9,10]. Natron-type glass is also known from 6th to 7th century Byzantine sites in the Eastern Mediterranean [11–13], Sicily [14] and Padua [15]. Glass of both natron and plant-ash type was found in the 8th–10th century site of Carvico in Northern Italy [16] and in a broad area of the Venetian lagoon (glass samples dating between the 7th and 13th century) [17]. The introduction of halophytic plant-ash that started at the end of the 8th/beginning of the 9th century was probably completed in the 13th century [18], which coincides with the development of Venice into a strong glass production centre.

Sites containing both natron and halophytic plant-ash glass are at present rare. Analysis of glass from the 6th and the end of the 8th to the beginning of the 10th century site of Gradišče above Bašelj in Slovenia showed it was all natron-type, except for two glass beads that were made of glass produced from the ash of halophytic plants [19]. Glass beads very likely spread faster than any other glass items. A few examples of plant-ash glass beads were also encountered among the early medieval beads from Strömkendorf in northern Germany [20].

Glass beads are an important time indicator, and therefore we designed an investigation of 97 glass beads found in cemeteries from the 7th to beginning of the 11th century in Slovenia (Fig. 1). They included six mosaic beads with eye decoration

* Corresponding author at: Faculty of Mathematics and Physics, University of Ljubljana, Jadranska 19, SI-1000 Ljubljana, Slovenia. Tel.: +386 1 4766589; fax: +386 1 2517281.
E-mail addresses: ziga.smit@ijs.si, ziga.smit@fmf.uni-lj.si (Ž. Šmit).

0168-583X/$ - see front matter © 2012 Elsevier B.V. All rights reserved.
doi:10.1016/j.nimb.2012.01.044

Fig. 1. Earrings with beads, necklaces and mosaic beads with eye decoration included in the study. Sites: Brda near Bled (1,3:), Pristava near Bled, graves 65, 141, 192 (2, 4, 5), Bela Cerkev near Šmarjeta (6), Pržan near Ljubljana (7, 8).

(*millefiori*, *Mosaikaugenperlen*) and several drawn-segmented and drawn-cut beads that often occur in graves together with mosaic beads. In archaeological publications, several types of such beads are regarded as being of oriental origin and are dated to the end of the 8th, and especially to the first half of the 9th century [21–24].

The beads included in the analysis came from sites that on archaeological grounds belong to two cultural groups. The first group, dated to the end of the 8th and to the 9th century, is represented by cemeteries in eastern Slovenia, for which pottery grave goods are characteristic [25]. The second group is the Köttlach culture in central Slovenia. Central European scholars date its beginning, i.e. its earliest stage (*Vor-Köttlach-Horizont*) to the first half of the 9th century and its later stages (*Köttlach I and II*) from the second half of the 9th to the first half of the 11th century [26]. In contrast, Slovenian archaeologists date its beginning (which they describe as the Caranthanian cultural group) earlier, i.e. to the 7th and 8th century, and its later stages (Köttlach cultural group in the narrow sense) to the 9th and 10th century [27].

2. Experimental

Analysis was performed at the Tandetron accelerator of the Jožef Stefan Institute in Ljubljana, using a proton beam in air. The method of proton-induced X-ray emission (PIXE) was used for analysis of elements heavier than silicon. The nominal proton energy was 3 MeV, which was reduced to approximately 2.7 MeV at the target, after passing an 8 μm Al window and a 1 cm air gap. A Si(Li) X-ray detector of 160 eV resolution at 5.89 keV was positioned at 45° with respect to the target normal. The air gap between the detector and target was 5.7 cm. The experimental geometry was maintained by nylon spacers; these replaced the previously used metal spacers made from nickel-plated needles, as the scattered protons also excited nickel atoms in the needles, thus worsening the detection limit for nickel to about 0.1%. Precise values of the air gaps were determined by measurements of a series of single-element and simple chemical compound targets, exploiting the signal from air argon for normalisation.

Two sequential measurements at the same spot were performed, one using the air gap as the only absorber, and the other using an additional absorber of 0.1 mm Al foil. The beam profile was approximately Gaussian, with 0.8 mm full width at half maximum (FWHM) at the target. The proton current was a few tenths of a nA for the first measurement and about 1 nA for the other, and the measuring time was 300–500 s. In this way we increased the sensitivity for mid-Z elements around Sr to about 10 μg/g. Spectral de-convolution was performed by the AXIL program and the two sets of X-ray intensities were combined into one using the Fe Kα line for normalisation.

As silicon was the lightest element detected, the concentrations of the essential glass elements Na, Mg and Al were determined from the yields of excited gamma rays (PIGE). A 2 μm thick Ta foil was used for the exit window, in order to reduce the background gamma radiation to sub-100 keV energies. The Ta foil was not used for X-ray measurements, as its M and L X-rays, which reached the detector on account of scattering in the air, would coincide with the X-rays of silicon and copper, respectively, from the target. The number of incident protons was measured by a thin wire mesh intersecting the beam before the exit foil. The transmission of the mesh was about 58% [28]. This type of measurement appeared more efficient than monitoring of silicon gamma lines, as their intensities decrease rapidly at proton energies below 3.1 MeV [29]. For example, at 2.4 MeV, production of the 1779 keV line in silicon is 36-times weaker than in aluminium [30].

The induced gamma rays were detected by a 40% efficiency intrinsic Ge detector. Gamma lines, produced by inelastic proton scattering, were observed at 440 keV for Na, 585 keV for Mg, and 844 and 1014 keV for Al. The latter two lines are also produced by a (p, γ) reaction in magnesium, though its contribution at energies above 1.7 MeV is negligible [30]. We also measured the count rate of the natural gamma line at 583 keV that coincides with the Mg line. As a result of the lead shielding of the detector and a sufficient count-rate of the proton-induced gamma rays, its intensity was below 10% of the Mg line induced in plant-ash glass, but of comparable intensity in the natron-type glass. The detection limit for MgO was thus estimated to be about 0.3%. For PIGE measurements, the proton current used was ~3 nA and the accumulated dose was 3 μC. A higher dose of 12 μC was used for the NIST 620 glass standard, which served for calibration. The gamma ray intensities were determined by the GRILS program of the GANAAS package.

The evaluation of elemental concentrations was made by an iterative procedure, considering the induced X-ray and gamma ray intensities simultaneously. The concentrations of Na, Mg and Al were calculated by the surface approximation [31], except that the necessary stopping power data were included iteratively, in the same way as the matrix effects for the induced X-rays. The elements were assumed to be in oxide form, and the sum of oxides was normalised to unity. As the shape of the beads departed considerably from the plane geometry assumed in the evaluation program, the following procedure was applied: The contents of Na_2O, MgO and Al_2O_3 obtained by PIGE were not re-normalised, as the more penetrative gamma rays did not attenuate in the target. The measured proton doses were further regarded as reliable, since any mishit of the proton beam for small beads was monitored by a scintillator positioned behind the target. From the total content of Na, Mg and Al oxides the code calculated the fraction of remaining metal oxides and normalised the concentrations obtained from the X-ray intensities to this value. However, the actual oxide sum could also be monitored with respect to the intensity of the Ar line in air, which measured the proton number for PIXE measurements. The distribution of these values is quite broad (Fig. 2), though it peaked at 0.9, i.e. close to unity.

By simulation, using a variable set of input parameters in the calculation, we found that the reason for this distribution is geometrical. As a test we chose a measurement with the sum of non-normalised oxide concentrations of 0.6, roughly exceeding the range of the left peak in Fig. 1. A unit sum was obtained by increasing the air gaps travelled by protons and X-rays by 2.1

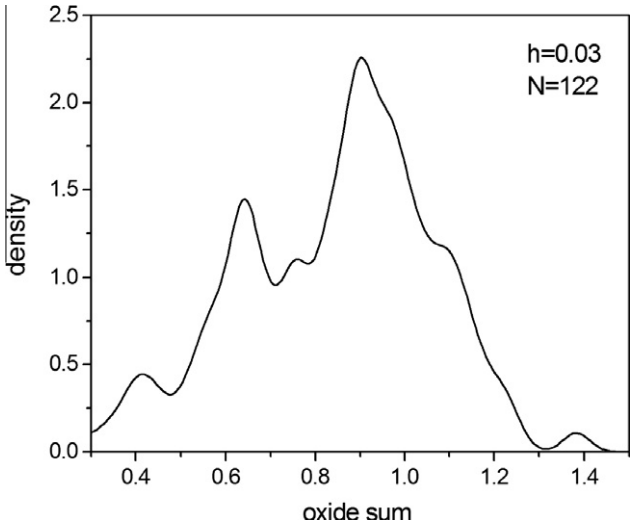

Fig. 2. Sum of metal oxides before re-normalisation, kernel-density estimate with $h = 0.03$.

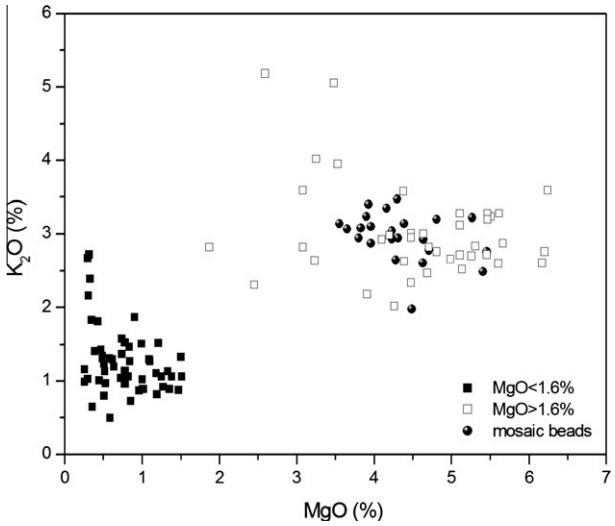

Fig. 4. Position of mosaic beads with eye decoration in the MgO – K_2O plot.

and 2.6 mm, respectively, or by strengthening the X-ray attenuation in the target itself, which we achieved by switching the X-ray take-off angle from 45° to 64°. As the accuracy in positioning of the targets was better than 0.5 mm, the second effect, geometrically modified X-ray attenuation in the target, was a much more probable case. A stronger X-ray attenuation in the target is consequence of longer X-ray escape lengths. Their increase is not only produced by a larger take-off angle, but is also result of surface roughness [32]. Surfaces of several beads were noticeably rough. The modelled increase of the take-off angle of 19°, appearing excessive at a glance, actually accounts for two effects: improper target tilting and surface roughness. The two effects are responsible for the significantly larger concentration uncertainties than for flat glass samples, which we typically quoted as ± 5% for major components [33]. Our model calculation revealed 22% variation of K and Ca concentrations, a few percent (2–4%) variations for Fe and Si, and 29% for Ag. Since this example approached an extreme case, typical concentration uncertainties for the majority of samples were 10–15%.

3. Results and discussion

The analysis included 91 beads from earrings and necklaces, and six mosaic beads with eye decoration (Fig. 1). The latter were composed of glass of various colours, which were analysed individually, making a total of 23 measurements on mosaic beads.

Several beads had a thick corrosion layer, which was carefully removed from an area of 2–3 mm^2, suitable for the measurement. Some beads had a rather rough or wrinkled surface, which contributed to strong X-ray attenuation. For the lightest elements, this deficiency was overcome using attenuation-independent PIGE, so unusually low Na_2O values were not encountered.

Plant ash contains more potassium and alkaline earth elements than natron, so the type of flux is unambiguously determined from the MgO–K_2O plot [7]. For the glass beads under discussion, the MgO–K_2O plot (Fig. 3) shows a compact natron group and a rather dispersed group of plant-ash glass. With respect to colour, some interesting observations could be made. All transparent beads are of natron-type glass (Fig. 3), suggesting they were made from old glass that circulated in the region and had been produced in the

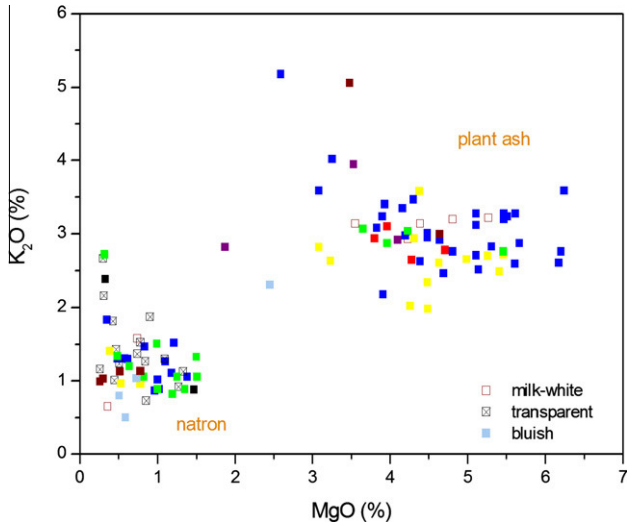

Fig. 3. MgO and K_2O contents (in weight%) in the beads analysed; colours resemble the actual colour.

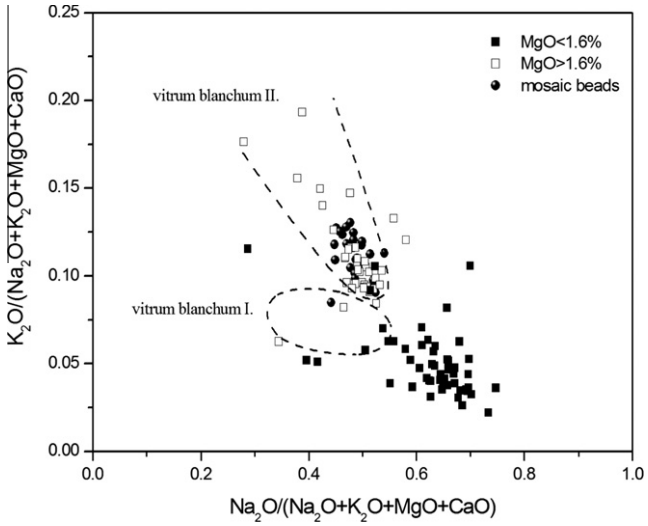

Fig. 5. Distribution of beads according to the relative contents of Na and K oxides. The contours display the two regions of Venetian *vitrum blanchum* glass [25,26].

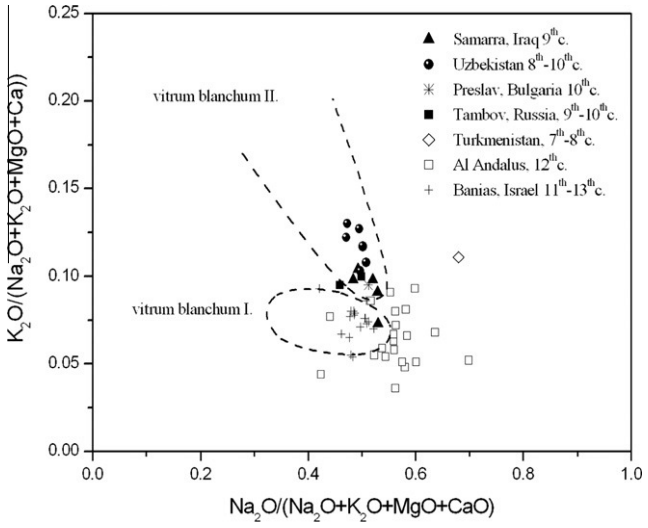

Fig. 6. Relative contents of Na and K oxides in selected glass samples from Islamic Spain [27] and the Levant [10], and from locations further east [28]. The contours show values for Venetian *vitrum blanchum* glass.

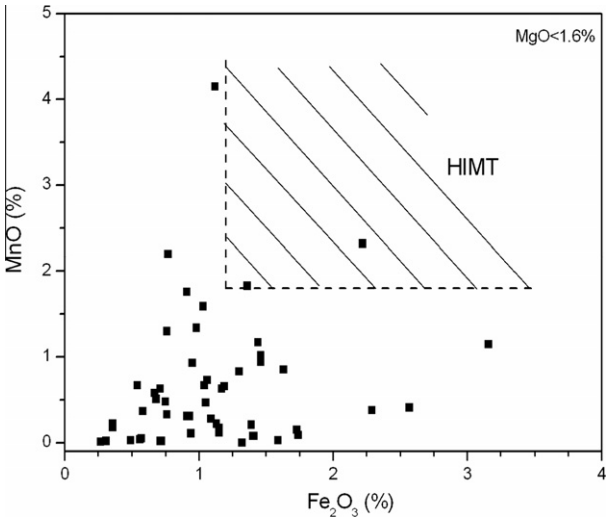

Fig. 8. The content of MnO versus Fe_2O_3 in natron-type glass, also showing the region of HIMT glass (hatched). The specimen with the highest MnO content contains 0.23% TiO_2.

(Late) Roman period. Milk-white, yellow, green, brown and blue beads belong to both types of glass. The red colour, which occurs only with mosaic beads, is only pertinent to plant-ash glass. Fig. 3 also shows, as expected, that the K_2O level is lower in the natron-type glass. But there are four samples that contain between 2 and 3% K_2O; a few examples of such glass were also detected among the glasses from Gradišče above Bašelj [19]. The MgO–K_2O plot, in which mosaic beads are shown by a special symbol, indicates that all mosaic beads were made of halophytic plants glass (Fig. 4).

Sources of plant-ash glass can be traced by plotting the relative fraction of Na_2O and K_2O in the total content of alkali and alkaline earth oxides [34]. In Fig. 5, the values for the samples under discussion are shown, as well as the range of values for Venetian white glass, which was similarly made from the ash of halophytic plants [35]. For the most numerous group of Venetian white glass, *vitrum blanchum I*, a relatively constant percentage of K_2O of about 8% is characteristic, while the minor group, *vitrum blanchum II,* exhibits an inverse correlation between sodium and potassium. This relation probably does not reflect intentional mixing of alkalis, but it may suggest use of different plant parts which contain various contents of alkalis [36]. Fig. 5 interestingly shows that most of the plant-ash glass beads fall with the group of *vitrum blanchum II*, which suggests the use of the same source of alkalis. It is known from written sources that the Venetians imported high-quality plant ash from the Levant (*alume catino*), while other European producers had to use other, less qualitative sources, such as *barilla* from Spain [34].

Particular alkali sources for *vitrum blanchum I* and *II* have not been identified. A suggestion for the alkali origin of *vitrum blanchum II* is provided in Fig. 6, which presents values for the relative fraction of Na_2O and K_2O in the total content of alkali and alkaline earth oxides for 12th century glass from Islamic Spain [37], 11th–13th century glass from the Islamic Levant [11] and 7th–10th century glass from different sites in the East [38]. It shows that *vitrum blanchum II* differs significantly from Mediterranean Islamic glass, suggesting that its alkali source should be sought further towards the (Middle)-East. This finding is supported by the stylistic analysis

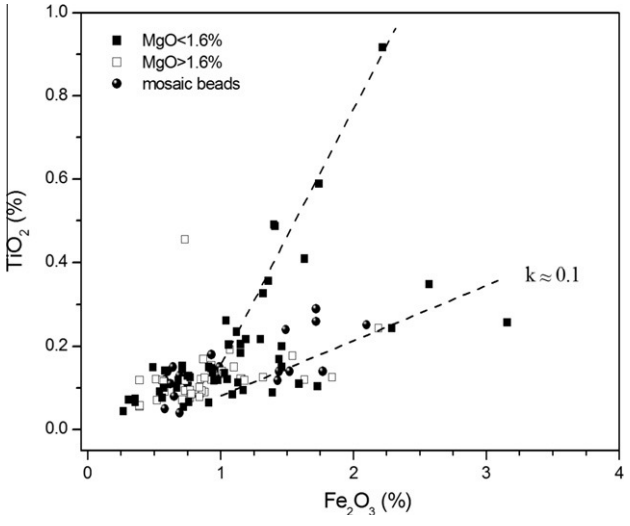

Fig. 7. Plot of Fe_2O_3 and TiO_2, showing the grade of purity of the siliceous sand.

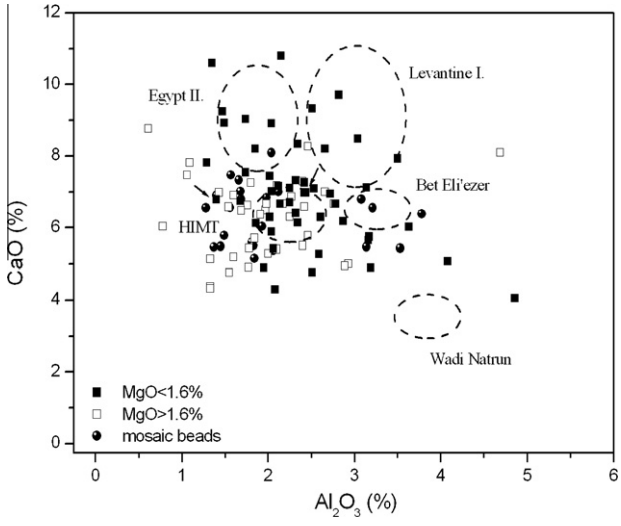

Fig. 9. Al_2O_3 versus CaO plot of the samples analysed and the regions of the five late and post-Roman groups of Levantine natron glass. Arrows show the two HIMT glasses identified in Fig. 8.

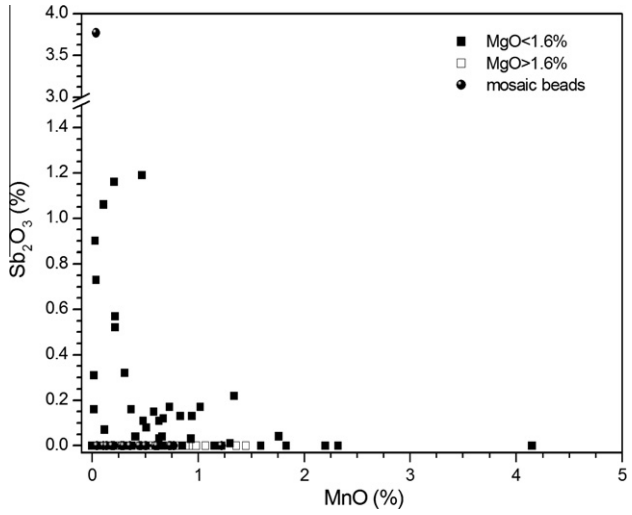

Fig. 10. Concentrations of the decolouring agents MnO and Sb_2O_3.

of Callmer, who proposed the origin of mosaic, drawn-segmented and drawn-cut beads in Iraq, more precisely the central part of the Caliphate [22].

Fig. 6 also shows similar values for *vitrum blanchum I* and Levantine Islamic glass, which is consistent with documented imports from the area. The glass from Islamic Spain is characterised by a much higher content of sodium, which might indicate a different purifying procedure of the flux; a similar alkali content appears in the glass that superseded *vitrum blanchum* [35].

The silicon sand, used as the source of silica, contained several other minerals as impurities, notably iron and titanium (Fig. 7). Most of the data in Fig. 7 are complex, i.e. they do not show a classification according to impurity level, though some natron-type glasses contain higher amounts of iron and titanium and even suggest the existence of two correlation lines, as observed in late Roman glass of San Martino di Ovaro [7] and in glass from the Venetian lagoon [16]. High Ti levels indicate more earth-like sediments, which were transported by large rivers such as the Nile, so the high Fe–Ti line might suggest natron-type glass produced in the Egyptian region [1].

Levels of TiO_2 above 0.4% may also indicate the so-called high-iron-manganese-titanium glass (HIMT), which can be assigned to the 4th–5th century workshops [39,1]. However, the Fe_2O_3–MnO plot (Fig. 8) shows that only two glass specimens (showing TiO_2 content of 0.36 and 0.92%, respectively) can be classified as HIMT glass; the content of MnO in the others is below 1%.

The origin of glass raw materials is further traced in the Al_2O_3–CaO plot (Fig. 9). In natron-type glass, calcium originates from the remnants of shells in siliceous coastal sand, while halophytic plant ash itself contains calcium [11]. The Al_2O_3–CaO plot (Fig. 9) does not show any correlation to the five late and post-Roman groups of natron-type glass of Levantine origin [1]. The values of Al_2O_3 are more dispersed than in the Levantine glass. For example, of the two HIMT glasses identified in Fig. 8, one falls within the HIMT

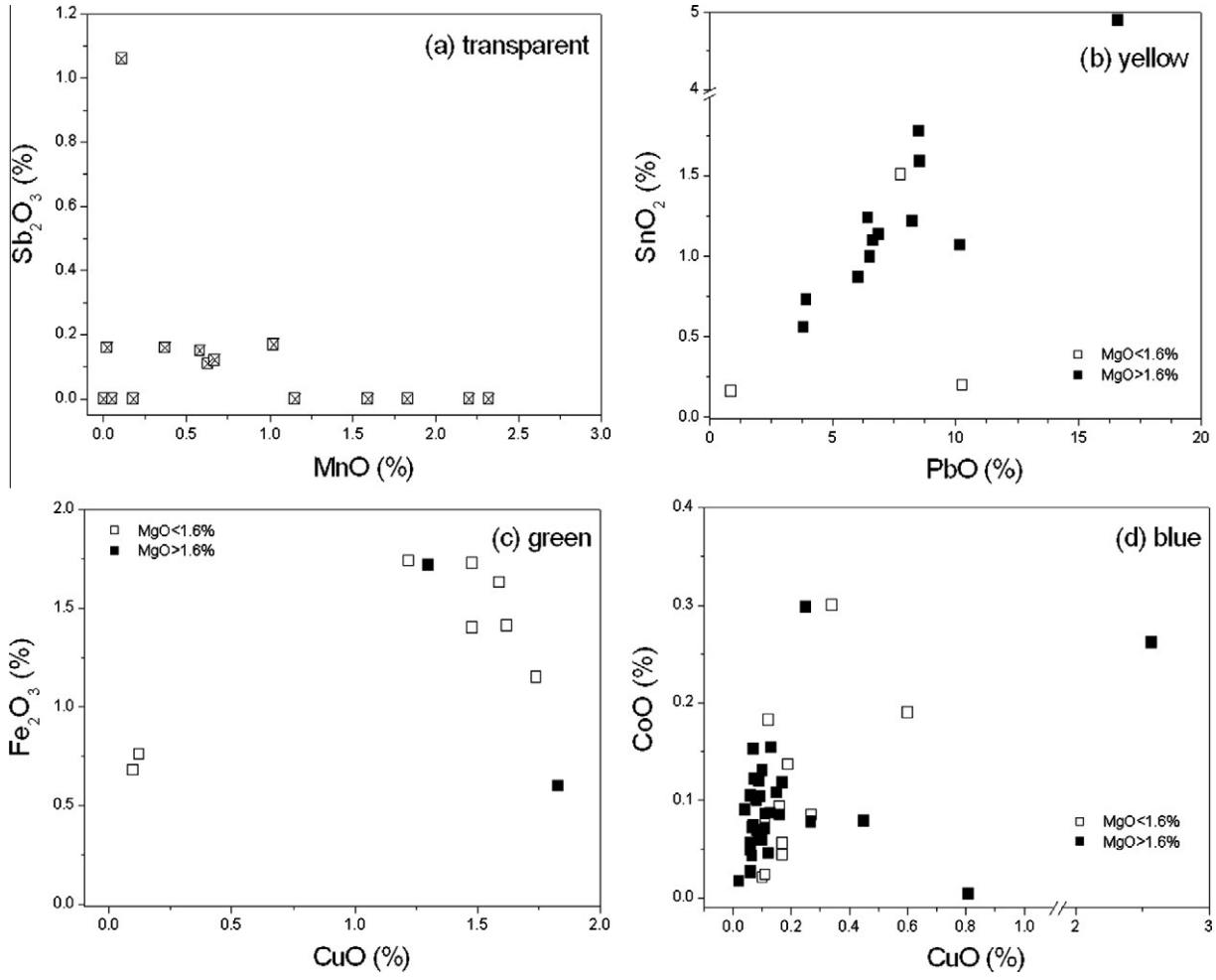

Fig. 11. Metal oxides used for glass (de)colouration in transparent (a), yellow (b), green (c) and blue glass (d).

boundaries of Fig. 9, but the other exhibits an Al_2O_3 content of 1.4%, which is lower than the HIMT group. Though our experimental errors implied significant data dispersion, Fig. 9 nevertheless suggests that the investigated glass beads exploited a variety of silica sources and that the materials might have also been mixed. Regarding CaO, two groups seem to appear. The upper one, centred at about 9% CaO, consists of (with one exception) natron-type glass. The lower group is centred at about 6% CaO and includes natron and plant ash glass. This finding is at first glance surprising as the plant-ash glass should also contain a CaO component from the ash. However, the lower CaO content reflects the change of silica source in the production of Islamic, i.e. plant ash glass [11]: coastal sand was replaced by crushed quartz with a significantly lower content of calcium. The CaO fraction in the glass was then actually that from the plant ash.

The content and isotopic composition of Sr is also characteristic of the source of calcium [1]. The content of SrO in the beads examined is higher than 280 μg/g, which is consistent with both coastal sand and plant-ash sources.

Decolouration of glass can be achieved by decolourisers such as antimony, manganese and arsenic oxides. In antiquity both antimony and manganese were used [3], while Venetian white glass contained only the latter [35]. These two agents could also be observed in the glass beads under discussion. Fig. 10 shows that Sb_2O_3 and MnO are in inverse correlation and that Sb_2O_3 appears only in natron-type glass.

Antimony was also used as a pigment, rather than decolouriser. In Fig. 11, the colouring oxides used for transparent, yellow, blue and green glass are shown. In transparent glass (Fig. 11a), only one sample has an Sb_2O_3 content of about 1%, whereas in all other samples it is lower than 0.2%. As Sb_2O_3 was not used in Roman glass after the 4th century AD [3,40], such low levels suggest gradual dilution of the agent in recycling processes. Beads with an Sb_2O_3 content between 0.2 and 1.2% (Fig. 10) are of different colours, so antimony may be either a residue of the previous decolouration process or was introduced in the pigmentation procedure. Tin, whose oxide SnO_2 has opacifying properties, was detected in all yellow-stained beads. The linear correlation between tin and lead (Fig. 11b) suggests that lead–tin yellow (lead stannate and/or lead tin oxide silicate) was used. Such a correlation was also observed in Merovingian beads [10]. A green colour was achieved with iron and copper compounds (Fig. 11c). A combination of copper and cobalt oxides was used for blue colouration (Fig. 11d). For a large fraction of values we can observe correlations between the two agents in both natron and plant-ash glass. A constant ratio between the two elements suggests long term use of the same recipe or pigment source.

4. Conclusions

The glass beads that circulated between the 7th–10th centuries in the area of present-day Slovenia were made from glass using either natron or plant ash as a flux. Among the 97 beads analysed, 57 were made of natron-type and 40 of plant-ash, the latter group being composed of 6 mosaic, 22 drawn-segmented and 12 drawn-cut beads. The natron glass may belong to Roman production. The new technology that used plant ash for glass production is clearly manifested in the mosaic beads with eye decoration, dated to the 9th century, as well as in the contemporary drawn-segmented and drawn-cut beads. Our results are in accordance with the recently published view that mosaic beads were of oriental origin and that the new glass technology developed in the Islamic and/or Byzantine world. We also suggest that the 8th–10th century glass probably exploited one of the two alkali sources that were used in Venetian and Venetian-like glass about 600 years later. In our opinion these sources were in the Near/Middle East, more precisely in Mesopotamia and around the Aral Sea.

The results have important implications for dating archaeologically established cultural groups. The cemeteries in eastern Slovenia, with characteristic ceramic grave goods, contained several glass beads made with the ash of halophytic plants, which most probably did not occur in central and western Europe before the beginning of the 9th century. This is well in accordance with the archaeological dating of the cultural group to the end of the 8th and to the 9th century. The situation regarding the Köttlach cultural group in central Slovenia is different. Beads made of halophytic plant ash glass originate from several graves assigned to the earliest subgroup of Köttlach cultural group, which Slovenian archaeologists date to the 7th and 8th century, but are dated later, i.e. to the first half of the 9th century, by central European archaeologists. The identification of halophytic plant ash glass makes a strong argument in favour of the later dating.

Acknowledgements

The authors would like to thank Mojca Vomer Gojkovič (Pokrajinski muzej Ptuj) and Borut Križ (Dolenjski muzej Novo mesto) for putting at their disposal many of the beads, and permission to make the analyses.

References

[1] I.C. Freestone, The Provenance of ancient glass through compositional analysis, Mater. Res. Soc. Symp. Proc. 852 (2005) 1–14.
[2] M.D. Nenna, M. Picon, M. Vichy, Ateliers primaires et secondaires en Égypte à l'époque Gréco-Romaine, in: M.D. Nenna (Ed.), La route du verre, TMO 33, maison d'Orient, Lyon, 2000, pp. 97–112.
[3] E.V. Sayre, R.W. Smith, Compositional categories of ancient glass, Science 133 (1961) 1824–1826.
[4] A. Shortland, L. Schachner, I. Freestone, M. Tite, Natron as a flux in the early vitreous materials industry: sources, beginnings and reasons for decline, J. Arch. Sci. 33 (2006) 521–530.
[5] Th. Rehren, A review of factors affecting the composition of early Egyptian glasses and faience: alkali and alkali earth oxides, J. Arch. Sci. 35 (2008) 1345–1354.
[6] B. Gómez-Tubío, M.Á. Ontalba Salamanca, I. Ortega-Feliu, M.Á. Respaldiza, F. Amores Carredano, D. González-Acuña, PIXE-PIGE analysis of late roman fragments, Nucl. Instr. and Meth. B 249 (2006) 616–621.
[7] A. Zucchiatti, L. Canonica, P. Prati, A. Cagnana, S. Roascio, A. Climent Font, PIXE-analysis of V-XVI century glasses from the archaeological site of San Martino di Ovaro (Italy), J. Cult. Herit. 8 (2007) 307–314.
[8] Ž. Šmit, T. Milavec, D. Jezeršek, Th. Rehren, unpublished.
[9] P. Hoffmann, S. Bichlmeier, M. Heck, C. Theune, J. Callmer, Chemical composition of glass beads of the Merovingian period from graveyards in the Black Forest, Germany, X-Ray Spectrom. 29 (2000) 92–100.
[10] F. Mathis, G. Othmane, O. Vrielynck, H. Calvo del Castillo, G. Chêne, T. Dupois, D. Strivay, Combined PIXE/PIGE and IBIL with external beam applied to the analysis of Merovingian glass beads, Nucl. Instr. and Meth. B 268 (2010) 2078–2082.
[11] I.C. Freestone, Y. Gorin-Rosen, M.J. Hughes, Primary glass from Israel and the production of glass in late Antiquity and the early Islamic period, in: M.-D. Nenna (Ed.), La route du verre, TMSO 33, maison d'Orient, Lyon, 2000, pp. 65–83.
[12] I.C. Freestone, M. Ponting, M.J. Hughes, The origins of Byzantine glass from Maroni Petrera, Cyprus, Archaeometry 44 (2002) 257–272.
[13] Th. Rehren, F. Marii, N. Schibille, L. Stanford, C. Swann, Glass supply and circulation in early Byzantine southern Jordan, in: J. Drauschke, D. Keller (Eds.), Glass in Byzantium – production usage analyses, RGZM, Mainz, 2010, pp. 65–81.
[14] R. Arletti, C. Giacobbe, S. Quartieri, G. Sabatino, G. Tigano, M. Triscari, G. Vezzalini, Archaeometrical investigation of Sicilian early Byzantine glass: chemical and spectroscopic data, Archaeometry 52 (2010) 99–114.
[15] R. Bertoncello, L. Milanese, U. Russo, D. Pedron, P. Guerriero, S. Barison, Chemistry of cultural glasses: the early medieval glasses of Monselice's hill (Padova, Italy), J. Non-Cryst. Solids 306 (2002) 249–262.
[16] M. Uboldi, M. Verità, Scientific Analyses of Glasses from Late Antique and Early Medieval Archaeological Sites in Northern Italy, J. Glass Stud. 45 (2003) 115–137.
[17] M. Verità, A. Renier, S. Zecchin, Chemical analyses of ancient glass findings excavated in the Venetian lagoon, J. Cult. Herit. 3 (2002) 261–271.
[18] M. Verità, S. Zecchin, Thousand years of Venetian glass: the evolution of chemical composition from the origins to the 18th century, Annales du 17e congrès de l'AIHV (Antwerp, Antwerp 2009 (2006) 602–613.

[19] Ž. Šmit, D. Jezeršek, T. Knific, J. Istenič, PIXE-PIGE analysis of Carolingian perod glass from Slovenia, Instr. and Meth. B 267 (2009) 121–124.
[20] M. Heck, Analysenbericht zu chemisch-analytischen Untersuchungen an frühmittelalterlichen Glasfunden aus Gross Strömkendorf, in: A. Pöche (Ed.), Perlen, Schwerin, Trichterglässer, Tesserae, 2005, pp. 203–215.
[21] R. Andrae, Mosaikaugenperlen. Untersuchungen zur Verbreitung und Datierung karolingzeitlicher Millefioriglasperlen in Europa, Acta Praehistorica et Archaeologica 4 (1973) 101–198.
[22] J. Callmer, Trade Beads and the Bead Trade in Scandinavia, ca 800–1000 AD, Lund, (1977), pp. 99.
[23] J. Callmer, Beads and Bead Production in Scandinavia and the Baltic Region, ca. AD 600–1100; a general outline. In: U. von Freeden, A. Eiczorek (Eds), Kolloquien zur Vor- and Frühgeschichte 1, Bonn (1997), 195–202.
[24] A. Pöche, Perlen, Trichterglässer, Tesserae. Spuren des Glashandels und Glashandwerks auf dem frühgeschichtlichen Handelsplatz von Gross Strömkendorf, Landkreis Nordwestmecklenburg. Beitrage zur Ur- und Frühgeschichte Mecklenburg-Vorpommerns 44, Schwerin (2005).
[25] S. Ciglenečki, T. Knific, Old Slavic cemetery at Zgornji Duplek – archaeological report, Arh. Vestnik 30 (1979) 473–482 (in Slovenian, English summary).
[26] J. Giesler, Zur Archäologie des Ostalpenraumes vom 8. bis 11. Jahrhundert, Archäologisches Korrespondenzblatt (Mainz) 10 (1980) 85–98.
[27] P. Korošec, Early medieval archaeological image of Karantanian Slavs, Works of the Slovenian Academy of Sciences 22, Ljubljana (1979) (in Slovenian, German summary).
[28] D. Jezeršek, Ž. Šmit, P. Pelicon, External beamline setup for plated target investigation, Nucl. Instr. and Meth. B 268 (2010) 2006–2009.
[29] A. Savidou, X. Aslanoglou, T. Paradellis, M. Pilakouta, Proton induced thick target γ-ray yields of light nuclei at the energy region Ep = 1.0–4.1 MeV, Nucl. Instr. and Meth. B 152 (1999) 12.
[30] J.-P. Hirvonen, R. Lappalainen, Particle-Gamma Data, in: J.R. Tesmer, M. Nastasi, (Eds.), Handbook of Modern Ion Beam Materials Analysis, Materials Research Society, Pittsburgh, 1995, p. 573–613.
[31] A. Climent-Font, A. Muñoz-Martin, M.D. Ynsa, A. Zucchiatti, Quantification of sodium in ancient Roman glasses with ion beam analysis, Nucl. Instr. and Meth. B 266 (2008) 640–648.
[32] Ž. Šmit, Surface roughness correction in thick target PIXE analysis, Nucl. Instr. and Meth. B 28 (1987) 567–570.
[33] Ž. Šmit, P. Pelicon, M. Holc, M. Kos, PIXE/PIGE characterization of medieval glass, Nucl. Instr. and Meth. B 189 (2002) 344–349.
[34] Ine de Raedt, Composition of 16th–17th century façon-de-Venise glass excavated in Antwerp and neighbouring cities, Ph.D. dissertation, University of Antwerp 2001.
[35] Ž. Šmit, F. Stamati, N. Civici, A. Vevecka-Priftaj, M. Kos, D. Jezeršek, Analysis of Venetian-type glass fragments from the ancient city of Lezha (Albania), Nucl. Instr. and Meth. B 267 (2009) 2538–2544.
[36] Ž. Šmit, K. Janssens, O. Schalm, M. Kos, Spread of façon-de-Venise glassmaking through central and western Europe, Nucl. Instr. and Meth. B 213 (2004) 717–722.
[37] N. Carmona, M. Angeles Villegas, P. Jiménez, J. Navarro, M. García-Heras, Islamic glasses from Al-Andalus. Characterisation of materials from a Murcian workshop (12th century AD, Spain), J. Cult. Herit. 10 (2009) 439–445.
[38] M.A. Bezborodov, Chemie und Technologie der antiken und mittelalterlichen Gläser, Mainz 1975.
[39] P. Mirti, A. Casoli, L. Appolonia, Scientific analysis of Roman glass from Augusta Praetoria, Archaeometry 35 (1993) 225–240.
[40] C.M. Jackson, Making colourless glass in the Roman period, Archaeometry 47 (2005) 763–780.